Supporting Information

A Nonheme Manganese(IV)-Oxo Species Generated in Photocatalytic Reaction Using Water as an Oxygen Source

Xiujuan Wu,[a] Xiaonan Yang,[a] Yong-Min Lee,[b] Wonwoo Nam,*[b] and Licheng Sun*[a,c]

[a] State Key Laboratory of Fine Chemicals, Dalian University of Technology (DUT), DUT-KTH Joint Education and Research Center on Molecular Devices, Dalian 116024, China
[b] Department of Chemistry and Nano Science, Center for Biomimetic System, Ewha Womans University, Seoul 120-750, Korea
[c] Department of Chemistry, Institution School of Chemical Science and Engineering, KTH Royal Institute of Technology, Stockholm 210044, Sweden

E-mail: sunlc@dlut.edu.cn (S.L.), wwnam@ewha.ac.kr (N. W.)

Table of Contents

Experimental Section

Experimental Section

Materials

All chemicals were purchased from Aldrich Chemical Co. and Alfa Aesar Co. and used without further purification unless otherwise indicated. Solvents were dried and distilled under Ar prior to use according to the standard methods.[1] All synthetic reactions were carried out under Ar atmosphere with standard Schlenk techniques. The compounds tris(2,2'-bipyridyl)ruthenium(II) chloride, $Ru^{II}(bpy)_3Cl_2$ and tris(2,2'-bipyridyl)ruthenium(III) perchlorate, $Ru^{III}(bpy)_3(ClO_4)_3$ were prepared according to literature methods.[2,3] Ligand BQCN (*N*,*N'*-dimethyl-*N*,*N'*-bis(8-quinolyl)cyclohexanediamine) and manganese(II) complexes, $Mn^{II}(CF_3SO_3)_2 \cdot 2CH_3CN$ and $Mn^{II}(BQCN)(CF_3SO_3)_2$ (**2**), were prepared by literature methods.[4-6] The synthesis of **2** was carried out in dry box. BQCN (0.47 mmol, 187 mg) and $Mn^{II}(CF_3SO_3)_2 \cdot 2CH_3CN$ (0.57 mmol, 247 mg) were dissolved in CH_3CN and stirred at ambient temperature overnight. The resulting solution was filtered and added to a large volume of Et_2O. The product was obtained as a brownish yellow solid with 85% yield (370 mg). $H_2{}^{18}O$ (97% ^{18}O-enriched) was purchased from Aladdin chemical company.

Instrumentation

UV-vis spectra were recorded on an Agilent 8453 diode array spectrophotometer equipped with a UNISOKU Scientific Instruments Cryostat USP-203A for low-temperature experiments. Electrospray ionization mass spectra (ESI-MS) were collected on a Thermo Scientific (San Jose, CA, USA) TSQ Quantum UItra instrument, by infusing samples directly into the source using a syringe pump. The spray voltage was set at 3.7 kV and the capillary temperature at 373 K. X-band EPR spectra were taken at 77 K using X-band Bruker EMX-plus spectrometer equipped with a dual mode cavity. Low temperature was achieved and controlled by liquid N_2. The experimental parameters for EPR spectra were as follows: Microwave frequency = 9.25 GHz, microwave power = 1.0 mW, modulation amplitude = 10 G, modulation frequency = 100 kHz. ^1H NMR spectra were measured with a Bruker DRX-400 spectrometer. Product analysis for photocatalytic oxidation reactions was performed with an Agilent Technologies 6890N gas chromatography (GC) and Agilent Technologies 5975C gas chromatography / mass spectrometer (GC-MS). pH measurements were performed with a Leici pH-Meter PHS-3C. Photoirradiation of the sample was performed by using the light source of an Aulight CEL-HXF 300/CEL-HXUV 300 xenon light source with an appropriate band-path filter ($\lambda > 420$ nm).

Photocatalytic generation of $[Mn(IV)(O)(BQCN)]^{2+}$ (1)

The photocatalytic generation of **1** was carried out in an Ar-degassed acetate buffer (pH 4.0, 50 mM) and MeCN (*v*/*v* 1:6) mixed solvent. The reaction solution (2.0 mL) containing catalyst **2** (1.0 mM), $[Ru^{II}(bpy)_3]^{2+}$ (0.50 mM), and $[Co^{III}(NH_3)_5Cl]Cl_2$ (5.0 mM) was exposed to irradiation of an Xe lamp light source (300 W) with a cut-off filter ($\lambda > 420$ nm) and stirred for 10 min at 273 K. The final reaction solution was directly filtered and investigated into the spectral changes in the UV-vis spectroscopy with a quartz cuvette (path length = 10 mm) at 273 K.

Chemical generation, characterization and reactivity study of 1

Chemical generation of **1** was examined by monitoring the spectral change in the UV-vis spectroscopy with a quartz cuvette (path length = 10 mm) at 273 K. **1** was chemically generated in the oxidation of **2** (1.0 mM) by strong one-electron oxidants, cerium(IV) ammonium nitrate ($[Ce^{IV}(NO_3)_6](NH_4)_2$; CAN, 4.0 mM) and $[Ru^{III}(bpy)_3]^{3+}$ (2.0 mM), in a deaerated acetate buffer (pH 4.0, 50 mM) and MeCN (*v*/*v* 1:6) mixed solvent at 273 K. The intermediate **1** formed in the oxidation of **2** (1.0 mM) by $[Ru^{III}(bpy)_3]^{3+}$ (2.0 mM) was directly characterized by ESI-MS and X-band EPR spectroscopic methods at low temperature, respectively. Reactivity studies for **1** in the oxidation of alcohol and sulfide were followed by monitoring UV-vis spectral changes of reaction solutions. Subsequently, appropriate amounts of substrates were added to the solution of **1** in a deaerated acetate buffer (pH 4.0, 50 mM) and MeCN (*v*/*v* 1:6) mixed solvent.

Product analysis

Reactions were run at least in triplicate, and data reported represent the average of these reactions. Products formed in the photocatalytic oxidation of organic substrates by **1** under an Ar atmosphere were analyzed by GC and GC-MS. Quantitative analyses were made on the basis of comparisons of peak integration between products and authentic samples by ^1H NMR and GC. The photocatalytic oxidation of organic substrates by **1** was carried out in an Ar-degassed phosphate buffer (pH 6.8, 50 mM) and MeCN (*v*/*v* 19:1) mixed solvent and an Ar-degassed acetate buffer (pH 4.0, 50 mM) and MeCN (*v*/*v* 19:1) mixed solvent, respectively. The reaction solution (5.0 mL) containing catalyst **2** (4.0×10^{-2} mM), $[Ru^{II}(bpy)_3]^{2+}$ (0.40 mM), organic substrates (alcohol or sulfide 20 mM) and $[Co^{III}(NH_3)_5Cl]^{2+}$ (20 mM) was exposed to irradiation of an Xe lamp light source (300 W) with a cut-off filter ($\lambda > 420$ nm) and stirred for 2 h at 298 K. The final reaction solution was extracted with CH_2Cl_2 for five times and dried with anhydrous Na_2SO_4. After removal of solvent, the products were characterized and quantified by ^1H NMR spectroscopy and GC. During the whole photocatalytic oxidation of substrates by catalyst **2**, a circulating water system was used to keep the temperature constant at 298 K.

Control experiments were carried out in a similar manner described above. When the photocatalytic oxidation of thioanisole by **1** was performed in mixed solvent, which was prepared by using $H_2{}^{18}O$ instead of $H_2{}^{16}O$, the ^{18}O-labeled methyl phenyl sulfoxide product was detected by GC-MS, indicating that the oxygen atoms in product were derived from water. The decay product of intermediate **1** obtained in the oxidation of benzyl alcohol or thioanisole by **2** was also characterized by UV-vis, ESI-MS and EPR spectroscopic methods.

Quantum yield measurement

The quantum yields (Φ) were calculated by the following equations:[7]

Φ = moles of organic product / moles of absorbed photons

moles of absorbed photons = $Pt\lambda / N_A hc$

where organic products are benzaldehyde or methyl phenyl sulfoxide obtained under the conditions of quantum yield measurements, P is the difference of light intensity between the blank and sample, t is the irradiation time, λ is wavelength number of the incident light, N_A is the Avogadro constant, h is the Planck constant, c is the speed of the incident light.

A deaerated phosphate buffer (pH 6.8, 50 mM) and MeCN (*v/v* 19:1) mixed solvent and a deaerated acetate buffer (pH 4.0, 50 mM) and MeCN (*v/v* 19:1) mixed solvent, containing Mn(II)(BQCN)(OTf)$_2$ **2** (4.0×10^{-5} M), substrates (2.0×10^{-2} M), and $[Co^{III}(NH_3)_5Cl]^{2+}$ (2.0×10^{-2} M) were used as the blanks, respectively. Each of blank solution with photosensitizer $[Ru^{II}(bpy)_3]^{2+}$ (4.0×10^{-4} M) was used as the sample, respectively. The blanks and samples were exposed to irradiation of an Xe lamp light source (300 W) with a 450 nm band pass filter (λ = 450 nm) and stirred for 10 min at 298 K. The light intensity passing through the blanks and samples were detected behind a quartz reactor with a CEL-NP 2000 laser power meter, respectively. The difference of the light intensity between blanks and samples were considered to be the absorbed photons by photosensitizer, $[Ru^{II}(bpy)_3]^{2+}$. The moles of the organic products were determined by GC and NMR under the conditions of quantum yields determination.

Owing to two photons are required for the two-electron oxidation of the substrates to produce one molecule of products, the ideal maximum quantum yield (Φ_{calcd}) should be 0.50. For benzyl alcohol, the experimental quantum yields were found to be 0.02 and 0.05 at pH 6.8

and pH 4.0, respectively. For thioanisole, the experimental quantum yields were found to be 0.15 and 0.26 at pH 6.8 and pH 4.0, respectively.

References

1. W. L. F. Armarego and C. L. L. Chai, *Purification of Laboratory Chemicals*, 6th edn., Pergamon Press, Oxford, U.K., 2009.
2. M. S. Lowry, W. R. Hudson, R. A. Pascal, Jr and S. Bernhard, *J. Am. Chem. Soc.*, 2004, **126**, 14129-14135.
3. P. K. Ghosh, B. S. Brunschwig, M. Chou, C. Creutz and N. Sutin, *J. Am. Chem. Soc.*, 1984, **106**, 4772-4183.
4. J. England, G. J. P. Britovsek, N. Rabadia and A. J. P. White, *Inorg. Chem.*, 2007, **46**, 3752-3767.
5. S. Groni, P. Dorlet, G. Blain, S. Bourcier, R. Guillot and E. Anxolabéhère-Mallart, *Inorg. Chem.*, 2008, **47**, 3166-3172.
6. S. C. Sawant, X. Wu, J. Cho, K.-B. Cho, S. H. Kim, M. S. Seo, Y.-M. Lee, M. Kubo, T. Ogura, S. Shaik and W. Nam, *Angew. Chem., Int. Ed.*, 2010, **49**, 8190.
7. (a) X. Li, M. Wang, D. Zheng, K. Han, J. Dong and L. Sun, *Energy Environ. Sci.*, 2012, **5**, 8220; (b) T. Lazarides, T. McCormick, P. Du, G. Luo, B. Lindley and Richard Eisenberg, *J. Am. Chem. Soc.*, 2009, **131**, 9192.

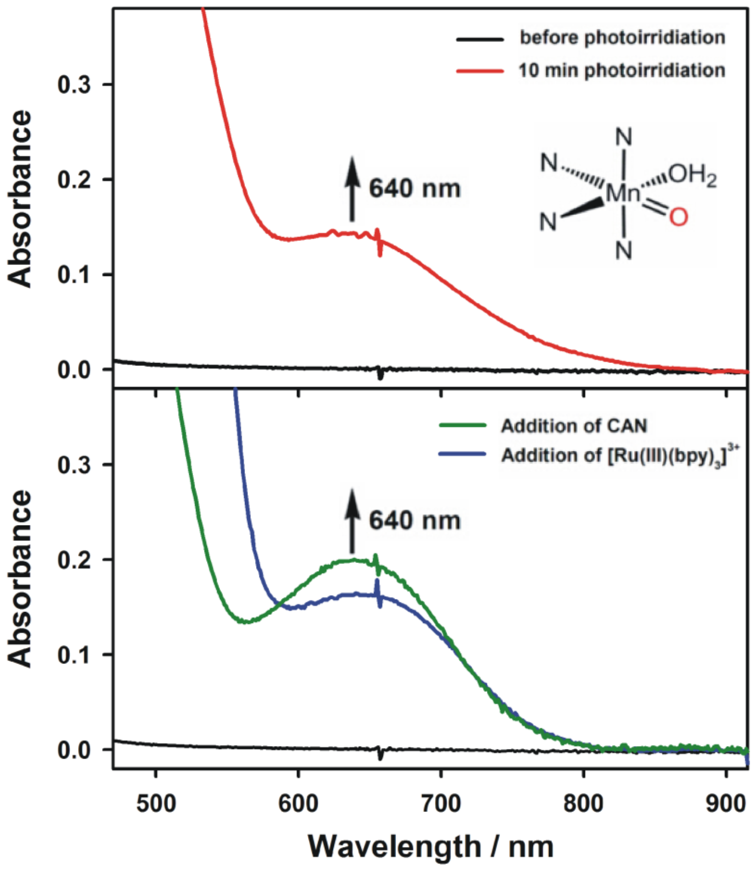

Fig. S1 UV-vis spectral changes showing the photocatalytic generation of **1** (red line) in the reaction of $[Ru^{II}(bpy)_3]^{2+}$ (0.50 mM), $[Co^{III}(NH_3)_5Cl]^{2+}$ (5.0 mM), and **2** (1.0 mM, black line) under photoirradiation ($\lambda > 420$ nm) (upper panel), and chemical generation in the oxidation reaction of **2** (1.0 mM; black line) by CAN (4.0 mM) (green line) and by $[Ru^{III}(bpy)_3]^{3+}$ (2.0 mM) (blue line) (lower panel), in a deaerated acetate buffer (pH 4.0, 50 mM) and MeCN (*v/v* 1:6) mixed solvent at 273 K, respectively.

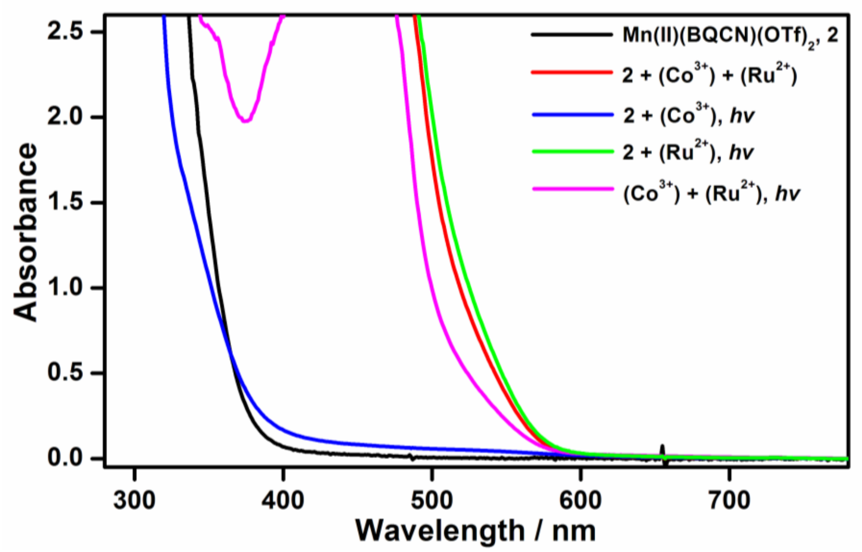

Fig. S2 Control experiments were performed in a deaerated acetate buffer (pH 4.0, 50 mM) and MeCN (*v*/*v* 1:6) mixed solvent at 273 K. UV-vis spectra obtained in the reaction of **2** (1.0 mM; black line), $[Ru^{II}(bpy)_3]^{2+}$ (Ru^{2+}, 0.50 mM) and $[Co^{III}(NH_3)_5Cl]^{2+}$ (Co^{3+}, 5.0 mM) without the photoirradiation (red line), and in the reaction of **2** with Co^{3+} (blue line), **2** with Ru^{2+} (green line) and Ru^{2+} with Co^{3+} (pink line) under the photoirradiation (λ > 420 nm), respectively.

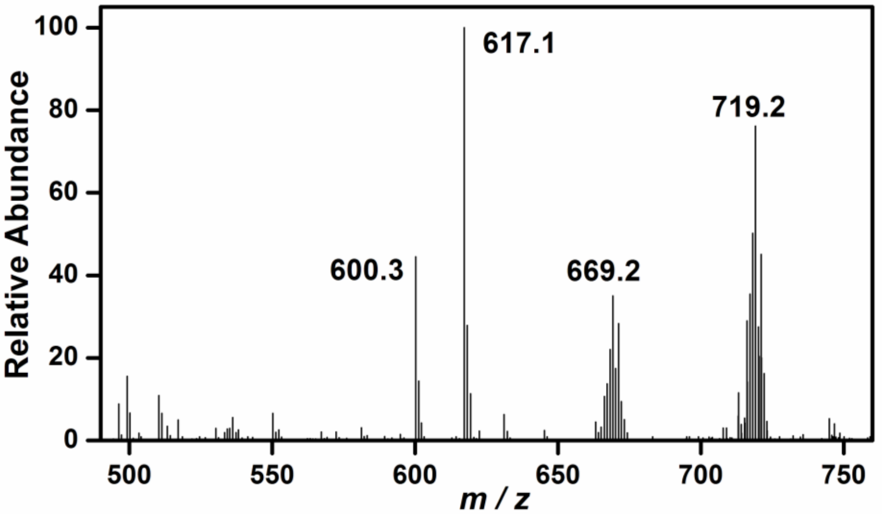

Fig. S3 ESI-MS spectrum of Mn^{III}(OH) species formed in a one-electron oxidation of **2** (1.0 mM) by [Ru^{III}(bpy)$_3$]$^{3+}$ (1.0 mM) in a deaerated acetate buffer (pH 4.0, 50 mM) and CH_3CN (*v*/*v* 1:6) mixed solvent at 273K. Peaks at *m*/*z* = 600.3, 617.1, 669.2, and 719.2 correspond to [Mn^{II}(BQCN)(CF_3SO_3)]$^+$ (calcd. *m/z* = 600.1), [Mn^{III}(OH)(BQCN)(CF_3SO_3)]$^+$ (calcd. *m/z* = 617.1), [Ru^{II}(bpy)$_3$(ClO_4)]$^+$ (calcd. *m/z* = 669.1) and [Ru^{II}(bpy)$_3$(CF_3SO_3)]$^+$ (calcd. *m/z* = 719.1), respectively.

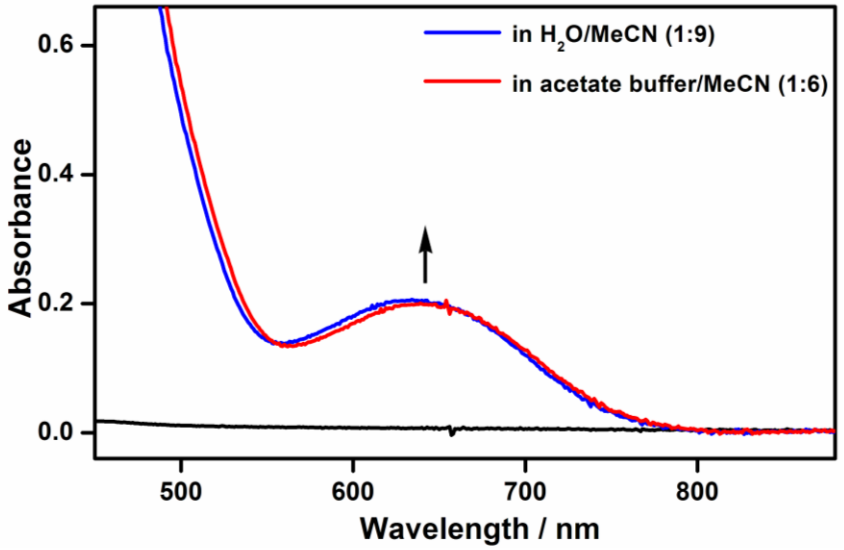

Fig. S4 UV-vis spectral changes showing the formation of **1** in the oxidation reaction of **2** (1.0 mM; black line) by CAN (4.0 mM) in a deaerated H_2O and MeCN (*v*/*v* 1:9) mixed solvent (blue line, λ_{max} = 630 nm), and a deaerated acetate buffer (pH 4.0, 50 mM) and MeCN (*v*/*v* 1:6) mixed solvent (red line, λ_{max} = 640 nm) at 273 K, respectively.

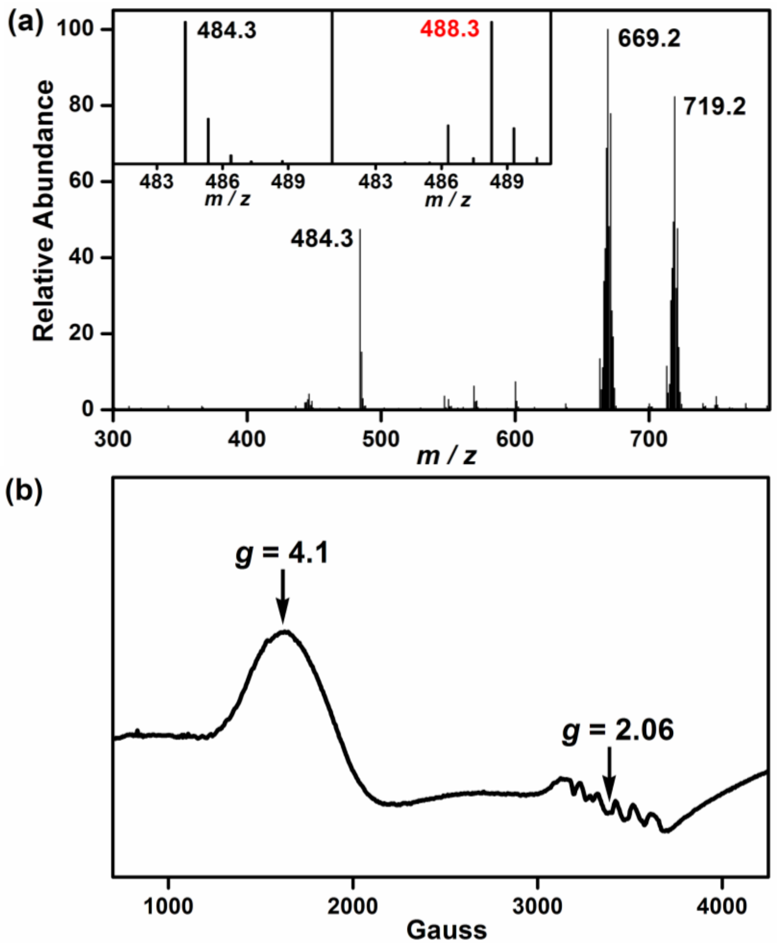

Fig. S5 Spectroscopic characterization of **1**, which was prepared in the reaction of **2** (1.0 mM) and $[\mathrm{Ru^{III}(bpy)_3}]^{3+}$ (2.0 mM) in a deaerated acetate buffer (pH 4.0, 50 mM) and MeCN (*v*/*v* 1:6) mixed solvent at 273K. (a) ESI-MS spectrum of **1**. Peaks at m/z = 484.3, 669.2 and 719.2 correspond to $[\mathrm{Mn^{IV}(O)(OH)(BQCN)}]^+$ (calcd. m/z = 484.2), $[\mathrm{Ru^{II}(bpy)_3(ClO_4)}]^+$ (calcd. m/z = 669.1) and $[\mathrm{Ru^{II}(bpy)_3(CF_3SO_3)}]^+$ (calcd. m/z = 719.1), respectively. Insets show the observed isotope distribution patterns for $[^{16}\mathrm{O}]$-**1** (left panel, prepared with $\mathrm{H_2{}^{16}O}$) and $[^{18}\mathrm{O}]$-**1** (right panel, prepared with $\mathrm{H_2{}^{18}O}$). (b) X-band EPR spectrum of **1** recorded at 77 K. The hyperfine splitting observed at g = 2.06 results from a minor impurity of Mn(II) species.

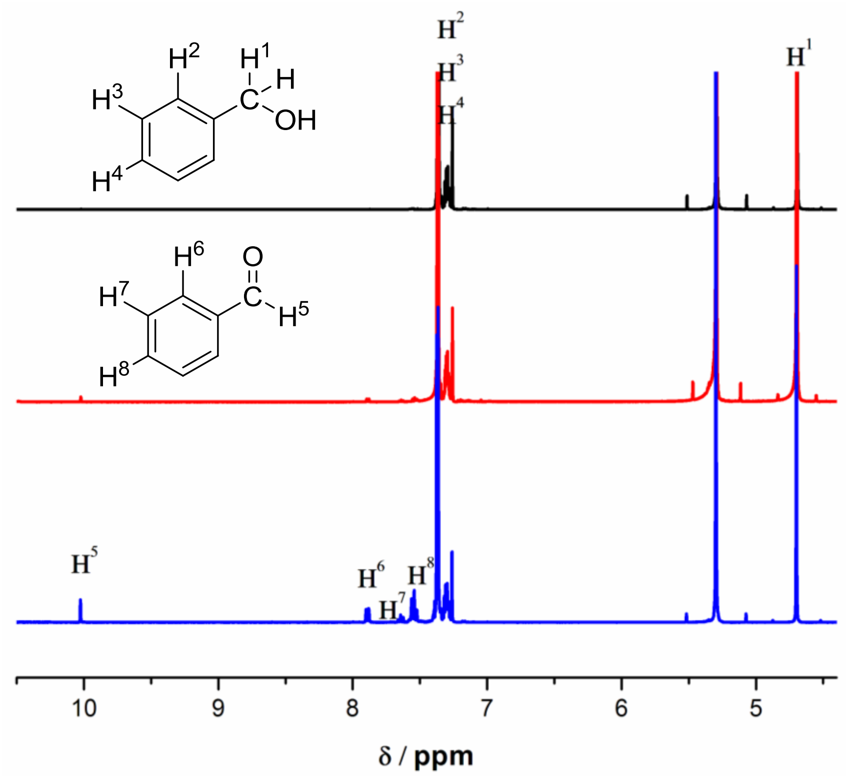

Fig. S6 ^{1}H NMR spectra of the reaction solution containing benzyl alcohol (20 mM), $[Ru^{II}(bpy)_3]^{2+}$ (0.40 mM) and $[Co^{III}(NH_3)_5Cl]^{2+}$ (20 mM) in the absence (red line) and presence (blue line) of catalyst **2** (4.0×10^{-2} mM) under photoirradiation ($\lambda > 420$ nm) for 2 h in deaerated phosphate buffer (pH 6.8, 50 mM) and MeCN (*v*/*v* 19:1) mixed solvent at 298 K. Black line shows ^{1}H NMR spectrum of reaction solution in the presence of catalyst **2** (4.0×10^{-2} mM) without photoirradiation under the same conditions.

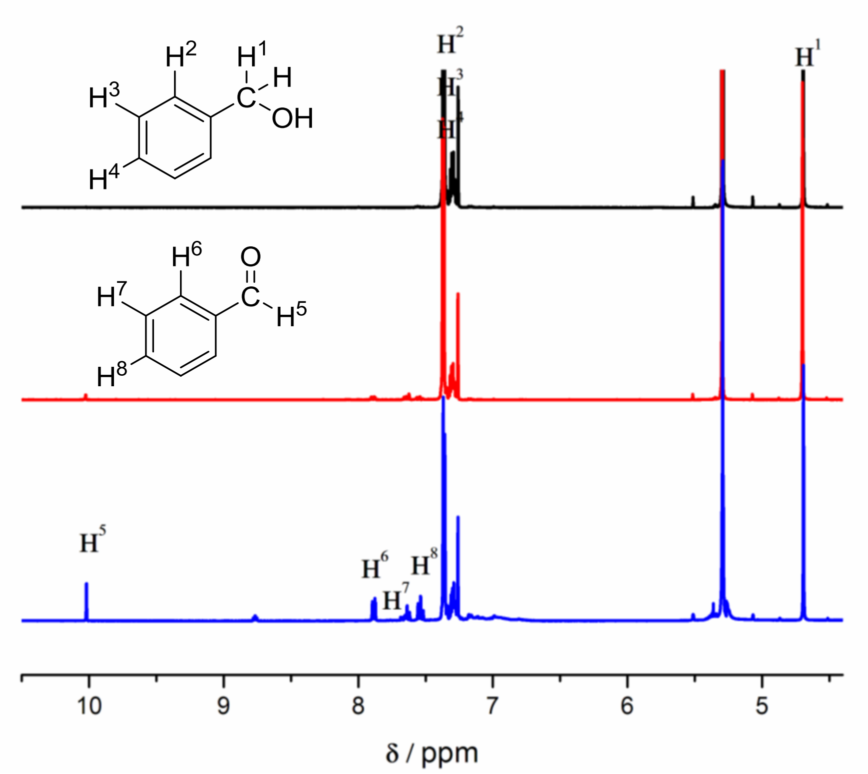

Fig. S7 ^{1}H NMR spectra of the reaction solution containing benzyl alcohol (20 mM), $[Ru^{II}(bpy)_3]^{2+}$ (0.40 mM) and $[Co^{III}(NH_3)_5Cl]^{2+}$ (20 mM) in the absence (red line) and presence (blue line) of catalyst **2** (4.0×10^{-2} mM) under photoirradiation ($\lambda > 420$ nm) for 2 h in deaerated acetate buffer (pH 4.0, 50 mM) and MeCN (*v*/*v* 19:1) mixed solvent at 298 K. Black line shows ^{1}H NMR spectrum of reaction solution in the presence of catalyst **2** (4.0×10^{-2} mM) without photoirradiation under the same conditions.

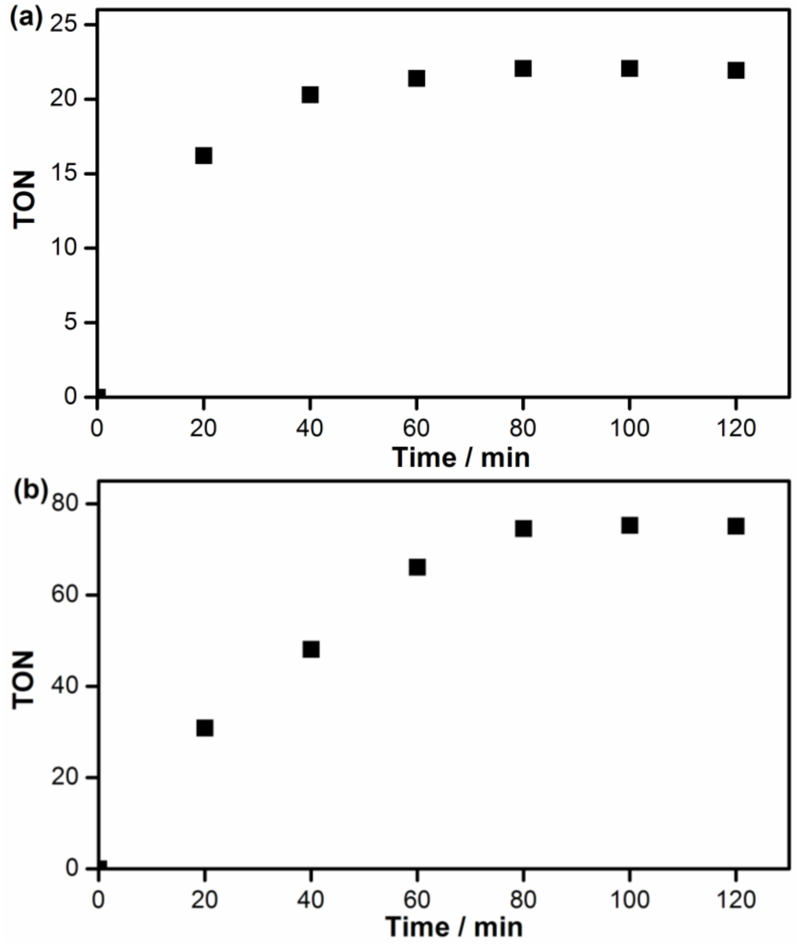

Fig. S8 Time profiles of turnover number (TON) in photocatalytic oxidation of benzyl alcohol as a substrate (20 mM) by catalyst **2** (4.0×10^{-2} mM) in the presence of $[\mathrm{Ru^{II}(bpy)_3}]^{2+}$ (0.40 mM) and $[\mathrm{Co^{III}(NH_3)_5Cl}]^{2+}$ (20 mM) under photoirradiation (λ > 420 nm) (a) in deaerated phosphate buffer (pH 6.8, 50 mM) and MeCN (*v*/*v* 19:1) mixed solvent and (b) in deaerated acetate buffer (pH 4.0, 50 mM) and MeCN (*v*/*v* 19:1) mixed solvent at 298 K.

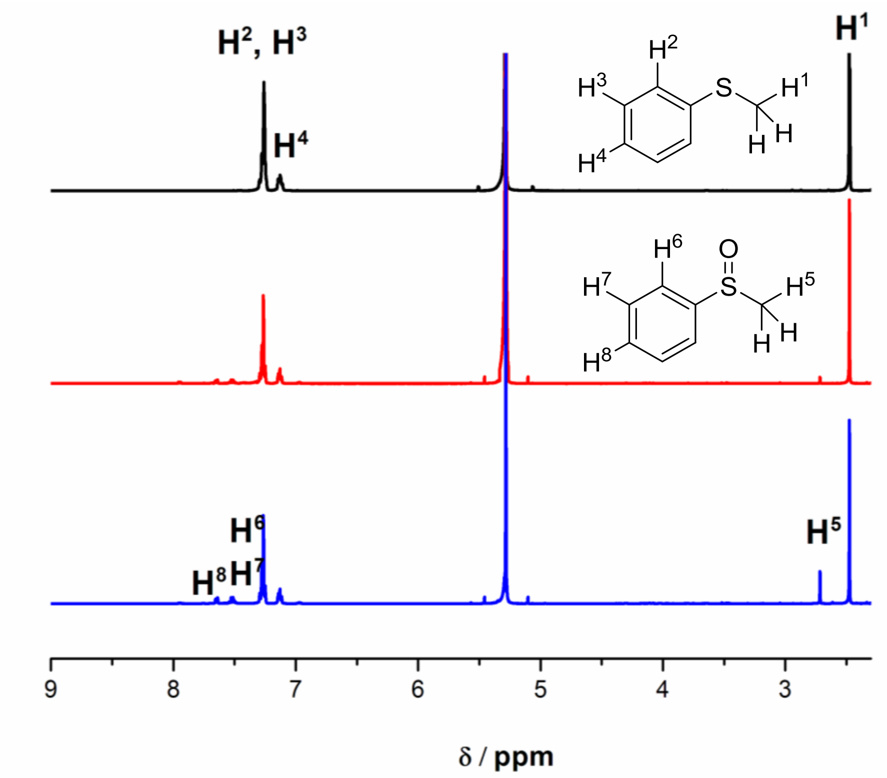

Fig. S9 ^{1}H NMR spectra of the reaction solution containing thioanisole (20 mM), $[\mathrm{Ru^{II}(bpy)_3}]^{2+}$ (0.40 mM) and $[\mathrm{Co^{III}(NH_3)_5Cl}]^{2+}$ (20 mM) in the absence (red line) and presence (blue line) of catalyst **2** (4.0×10^{-2} mM) under photoirradiation ($\lambda > 420$ nm) for 2 h in deaerated phosphate buffer (pH 6.8, 50 mM) and MeCN (*v*/*v* 19:1) mixed solvent at 298 K. Black line shows ^{1}H NMR spectrum of reaction solution in the presence of catalyst **2** (4.0×10^{-2} mM) without photoirradiation under the same conditions.

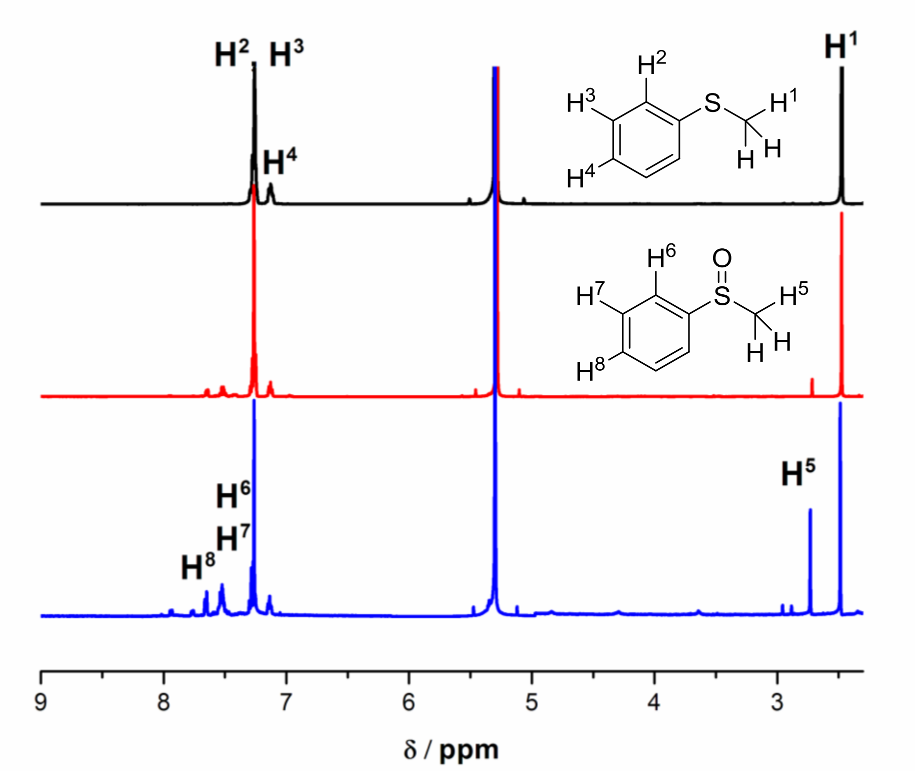

Fig. S10 ^{1}H NMR spectra of the reaction solution containing thioanisole (20 mM), $[Ru^{II}(bpy)_3]^{2+}$ (0.40 mM) and $[Co^{III}(NH_3)_5Cl]^{2+}$ (20 mM) in the absence (red line) and presence (blue line) of catalyst **2** (4.0×10^{-2} mM) under photoirradiation ($\lambda > 420$ nm) for 2 h in deaerated acetate buffer (pH 4.0, 50 mM) and MeCN (*v*/*v* 19:1) mixed solvent at 298 K. Black line shows ^{1}H NMR spectrum of reaction solution in the presence of catalyst **2** (4.0×10^{-2} mM) without photoirradiation under the same conditions.

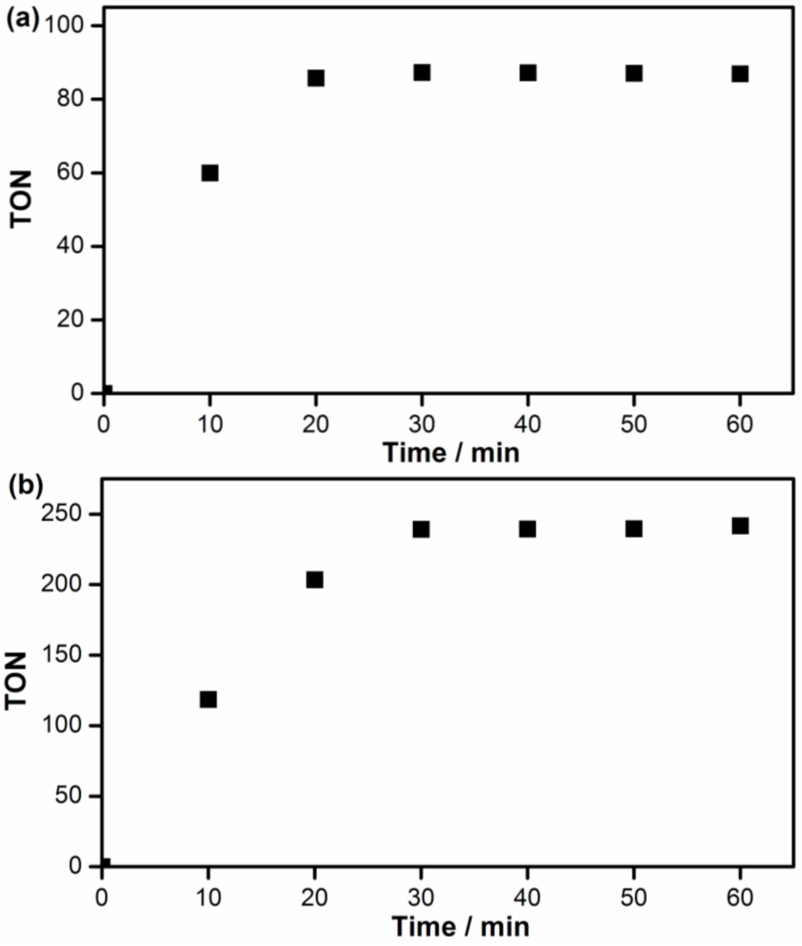

Fig. S11 Time profiles of turnover number (TON) in photocatalytic oxidation of thioanisole as a substrate (20 mM) by catalyst **2** (4.0×10^{-2} mM) in the presence of $[Ru^{II}(bpy)_3]^{2+}$ (0.40 mM) and $[Co^{III}(NH_3)_5Cl]^{2+}$ (20 mM) under photoirradiation ($\lambda > 420$ nm) (a) in deaerated phosphate buffer (pH 6.8, 50 mM) and MeCN (*v*/*v* 19:1) mixed solvent and (b) in deaerated acetate buffer (pH 4.0, 50 mM) and MeCN (*v*/*v* 19:1) mixed solvent at 298 K.

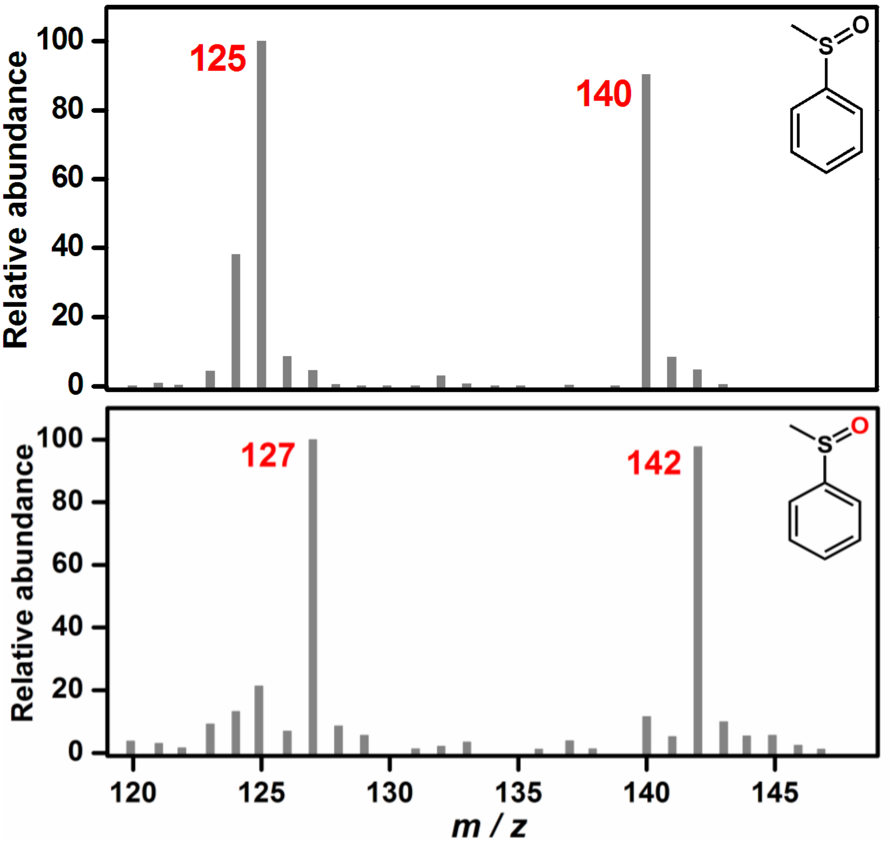

Fig. S12 GC-MS spectra of methyl phenyl sulfoxide formed in the photocatalytic oxidation of thioanisole (20 mM) by catalyst **2** (4.0 × 10^{-2} mM) in the presence of $[Ru^{II}(bpy)_3]^{2+}$ (0.40 mM) and $[Co^{III}(NH_3)_5Cl]^{2+}$ (20 mM) in a deaerated acetate buffer containing $H_2{}^{16}O$ (pH 4.0, 50 mM) and CH_3CN (*v*/*v* 19:1) mixed solvent (upper panel) and in a deaerated acetate buffer containing $H_2{}^{18}O$ (pH 4.0, 50 mM) and CH_3CN (*v*/*v* 19:1) mixed solvent (lower panel) under photoirradiation (λ > 420 nm) with a continously strring for 2 h at 298 K. The ^{18}O-compositions in product was determined by the comparison of the relative abundances of *m/z* = 125 and 140 for unlabeled methyl phenyl sulfoxide and *m/z* = 127 and 142 for ^{18}O-labeled methyl phenyl sulfoxide, respectively.

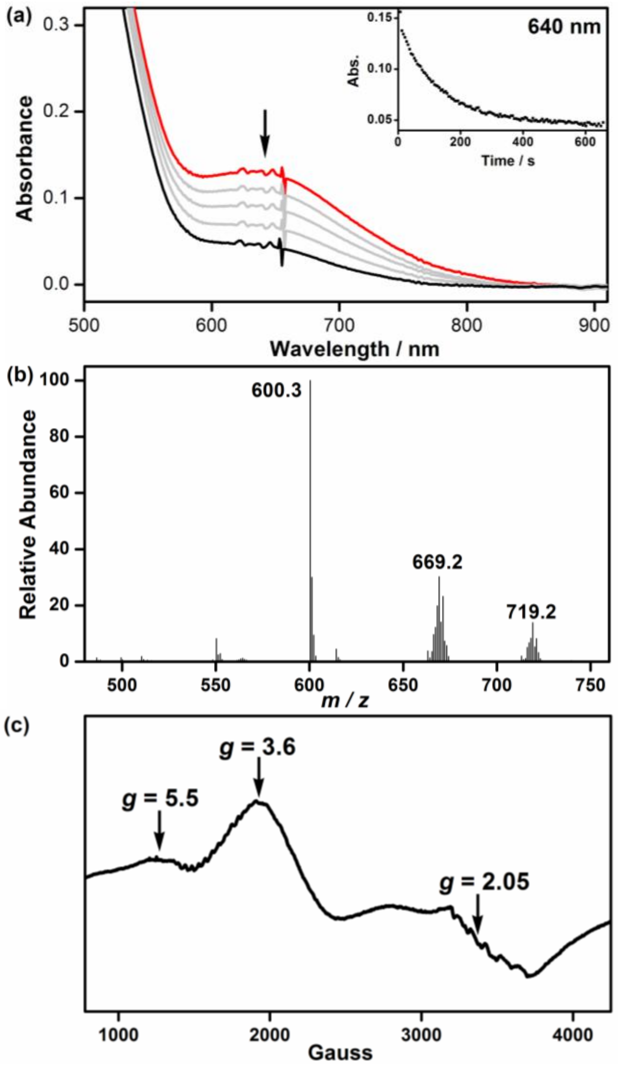

Fig. S13 (a) UV-vis spectral changes observed in the oxidation of thioanisole (50 mM) by **1** (red line), which was generated in chemical oxidation reaction of **2** (1.0 mM) by 2 equiv. of $[\mathrm{Ru^{III}(bpy)_3}]^{3+}$, in a deaerated acetate buffer (pH 4.0, 50 mM) and CH_3CN (*v*/*v* 1:6) mixed solvent at 273K. Inset shows the time course monitored at 640 nm due to **1**. (b) ESI-MS spectrum of reaction solution obtained in the oxidation of thioanisole (50 mM) by **1** (1.0 mM) under the same conditions of UV-vis spectroscopy. Peaks at m/z = 600.3, 669.2 and 719.2 correspond to $[\mathrm{Mn^{II}(BQCN)(CF_3SO_3)}]^+$ (calc. m/z = 600.1), $[\mathrm{Ru^{II}(bpy)_3(ClO_4)}]^+$ (calc. m/z = 669.1) and $[\mathrm{Ru^{II}(bpy)_3(CF_3SO_3)}]^+$ (calc. m/z = 719.1), respectively. (c) X-band CW-EPR spectrum of reaction solution obtained in the oxidation of thioanisole (50 mM) by **1** (1.0 mM) under the same conditions of UV-vis spectroscopy. Spectrum was recorded at 77 K.

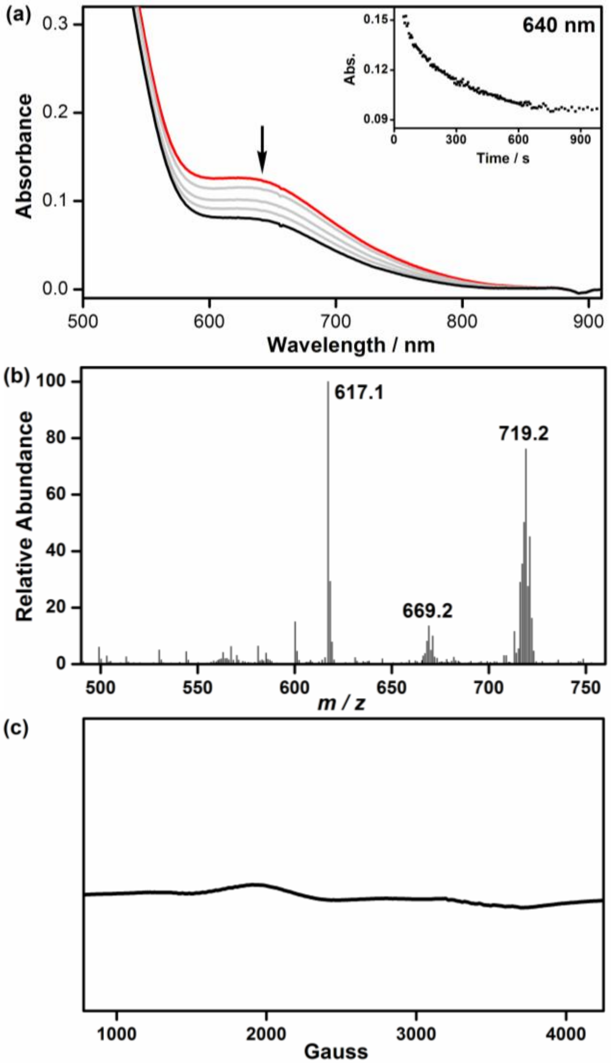

Fig. S14 (a) UV-vis spectral changes observed in the oxidation of benzyl alcohol (200 mM) by **1** (red line), which was generated in chemical oxidation reaction of **2** (1.0 mM) by 2 equiv. of $[Ru^{III}(bpy)_3]^{3+}$, in a deaerated acetate buffer (pH 4.0, 50 mM) and CH_3CN (*v*/*v* 1:6) mixed solvent at 273K. Inset shows the time course monitored at 640 nm due to **1**. (b) ESI-MS spectrum of reaction solution obtained in the oxidation of benzyl alcohol (200 mM) by **1** (1.0 mM) under the same conditions of UV-vis spectroscopy. Peaks at *m*/*z* = 617.1, 669.2 and 719.2 correspond to $[Mn^{III}(OH)(BQCN)(CF_3SO_3)]^+$ (calculated *m*/*z* 617.1), $[Ru^{II}(bpy)_3(ClO_4)]^+$ (calc. *m*/*z* = 669.1) and $[Ru^{II}(bpy)_3(CF_3SO_3)]^+$ (calc. *m*/*z* = 719.1), respectively. (c) X-band CW-EPR spectrum of reaction solution obtained in the oxidation of benzyl alcohol (200 mM) by **1** (1.0 mM) under the same conditions of UV-vis spectroscopy. Spectrum was recorded at 77 K.